Original Research

Feature article

Alteration of endothelial permeability ensures cardiomyocyte survival from ischemic insult in the subendocardium of the heart

Qing Chu[1*], Xin Song[1*], Ying Xiao[1] and Y James Kang[1,2] (iD)

[1]Regenerative Medicine Research Center, Sichuan University West China Hospital, Chengdu, Sichuan 610041, China; [2]Tennessee Institute of Regenerative Medicine, University of Tennessee Health Science Center, Memphis, TN 38163, USA
*These authors contributed equally to this paper.
Corresponding author: Y James Kang. Email: ykang7@uthsc.edu

Impact statement

Cardiomyocytes in the subendocardium can survive from ischemic insults. Understanding the mechanism by which these cells escape the fatal attack is critically important for strategic development to promote myocardial regeneration. This study reveals a preservation and transformation of endothelial cells in the subendocardial region, which allows blood infiltration under ischemic conditions. This in turn creates a unique microenvironment, leading to the survival of cardiomyocytes. This self-rescuing mechanism has significant implications for myocardial regeneration.

Abstract

Previous studies have shown that cardiomyocytes in the subendocardial region of myocardium survive from ischemic insult. This study was undertaken to explore possible mechanisms for the survival of these cardiomyocytes, focusing on changes in endothelial cells (ECs) and blood supply. C57/B6 mice were subjected to permanent ligation of left anterior descending (LAD) coronary artery to induce myocardial ischemia (MI). The hearts were harvested at 1, 4, and 7 days post MI and examined for histological changes. It was found that the survival of cardiomyocytes was associated with a preservation of ECs in the subendocardial region, as revealed by EC-specific *tdTomato* expression transgenic mice (*Tie2*[tdTomato]). However, the EC selective proteins, PECAM1 and VEGFR2, were significantly depressed in these ECs. Consequently, the ratio of PECAM1/tdTomato was significantly decreased, indicating a transformation from PECAM1^{+} ECs to PECAM1^{−} ECs. Furthermore, EC junction protein, VE-cadherin, was not only depressed but also disassociated from PECAM1 in the same region. These changes led to an increase in EC permeability, as evidenced by increased blood infiltration in the subendocardial region. Thus, the increase in the permeability of ECs due to their transformation in the subendocardial region allows blood infiltration, creating a unique microenvironment and ensuring the survival of cardiomyocytes under ischemic conditions.

Keywords: Myocardial ischemia, endothelial cells, cardiomyocytes, PECAM1, VE-cadherin, permeability

Introduction

Coronary artery occlusion dampens cardiac microvasculature network,[1,2] leading to massive loss of cardiomyocytes, except those in the subendocardial region of the myocardium.[3,4] The microvascular network supplies oxygen and nutrients to the heart and preserves the viability and normal function of cardiomyocytes.[5,6] We previously found that the survival of cardiomyocytes in the subendocardial region under ischemic conditions was associated with a remodeling of extracellular matrix (ECM).[3,7] In particular, a significant increase in lysyl oxidase (LOX), a copper-dependent amine oxidase catalyzing the cross-linking of collagens, was involved in the ECM remodeling. The ECM remodeling made an electrical disconnection between the surviving cardiomyocytes. Inhibition of LOX disturbed the ECM remodeling and reduced the surviving cardiomyocytes under ischemic conditions.[3]

Endothelial cells (ECs) are major vascular constituents and necessary for the transport of oxygen and nutrients.[8,9] Coronary artery occlusion leads to profound changes in microvascular and EC functions.[10] In the clinical approach, intra-arterial thrombolysis is the most efficient way to improve the ischemic microenvironment and to rescue injured cardiomyocytes from acute myocardial ischemia (MI).[11] At present, revascularization is considered to be one of the most important methods to promote myocardial regeneration.[12] Co-transplanting micro-vessels and pluripotent stem cell–derived cardiomyocytes helps cardiomyocyte survival in the ischemic myocardium.[13] It is, therefore, worthwhile that exploring changes in the microvascular network may be relevant to cardiomyocyte survival in the subendocardial region.

The dynamic changes in ECs reflect the alteration in several functional proteins, such as platelet EC adhesion

molecule 1 (PECAM1).[14,15] PECAM1 is involved in the regulation of EC adhesion to form a consecutive endothelial barrier.[14] PECAM1 deficiency impairs the integrity of EC junctions, facilitating EC transformation and increasing vascular permeability.[14,16] In addition, the type 2 receptor for vascular endothelial growth factor (VEGFR2) is involved in EC proliferation and migration. VEGFR2 mediates VEGF signaling cascades, activating DNA duplication and cell division.[17] In response to ischemic insult, these functional proteins in ECs are altered, resulting in EC activation as well as transformation, and myocardial microvascular remodeling.

This study was undertaken to explore changes in ECs in response to ischemic insult and their relation to cardiomyocyte survival in the subendocardial region. We found that ECs underwent a transformation, leading to an increase in their permeability, and allowing blood infiltration to constitute a unique microenvironment. This likely contributes to the survival of cardiomyocytes in the subendocardial region.

Materials and methods

Animal and animal care

Male C57/B6 mice (8–10 weeks old, weighing 18–22 g) were obtained from Chengdu Da-Shuo Experimental Animal Breeding and Research Center (Sichuan, China). *Tie2*[tdTomato] mice were achieved by crossing *Tie2-Cre* mice (Jackson's laboratory, JAX No. 008863) with *Rosa26-tdTomato* mice carrying the *loxP*-flanked ("floxed") stop cassette-controlled fluorescent marker *tdTomato* gene. Mice were fed standard chow (5C02, LabDiet, USA) and tap water *ad libitum*. Mice were acclimated to the experimental conditions for at least 1 week before surgery. All animal procedures were approved by the Institution Animal Care and Use Committee (IACUC) at Sichuan University, West China Hospital, following the guidelines of the US National Institutes of Health.

Genotypic identification

The tails of the transgenic mice were excised at the age of 6 to 7 weeks for DNA extraction. Genotyping was then performed by a standard PCR method using *Cre*-positive primers (5′-CACCCTGTTACGTATAGCCG-3′; 5′-GAGTCATCC TTAGCGCCGTA-3′), *Cre*-negative primers (5′-CCTAGGCACCAGGGTGTGAT-3′; 5′-TCACGGTTGGCCTTAGGGTT-3′), and *tdTomato* primers (pr1590: 5′-AAGGGAGCTGGCAGTGGAGTA-3′; pr1591: 5′-CCGAAAATCTGTGGGAAGTC-3′; pr1592: 5′-GGCATTAAAGCAGCGTATCC-3′; pr1593: 5′- CTGTTCCTGTACGGCATGG-3′).

Mouse model of MI

C57/B6 mice were randomly divided into sham-operated (*n* = 45) and MI (*n* = 66) groups. After genotyping the *Tie2*[tdTomato] mice, the positive mice were also randomly divided into sham (*n* = 3) and MI (*n* = 6) groups. The MI group was subjected to left anterior descending (LAD) artery ligation as described previously.[3] Briefly, mice underwent open chest surgery after anesthesia by isoflurane inhalation.

The LAD was exposed, and a 7-0 suture was pierced beneath. Then, the LAD was ligated to induce MI, and the mice revived shortly after sternal closure. The sham group underwent the same procedure as the MI group, except for LAD ligation. Of these mice, 112 survived until the time of sacrifice, including 105 C57/B6 mice and 7 *Tie2*[tdTomato] mice, and these mice were used for further investigations.

Tissue preparation

Mice were deeply anesthetized with isoflurane (5%) inhalation and euthanized in a CO_2-rich cage. Heart samples were collected for histological analysis. Briefly, the chests were opened, and the hearts were removed immediately. After washing in precooled saline (4°C), the atria were removed. For histological analysis, the hearts of mice were dissected along the ligature, embedded in optimal cutting temperature compound gel (Leica, Germany), and frozen in liquid nitrogen for serial frozen sections. The tissues were sectioned at 4 μm intervals and stored at –20°C for immunofluorescence staining. The remaining hearts were fixed in 4% paraformaldehyde, dehydrated in gradient alcohol, embedded in paraffin, and then cut into 2.5 μm sections for hematoxylin and eosin (HE) staining.

Hypoxyprobe detection

The hypoxyprobe-1 Omni kit (Hypoxyprobe, USA) was used to detect the oxygen content in the myocardium after ischemic injury according to the manufacturer's protocol. Hypoxyprobe-1 is widely used to detect hypoxic conditions in animal models. Once injected into an animal, the probe is rapidly distributed to all tissues in the body, while it only forms an adduct with proteins in cells that have O_2 concentrations < 14 μM (equivalent to a partial oxygen pressure of 10 mmHg at 37°C). One hour before sacrifice, the mice were intraperitoneally injected with a 10 mg/mL solution (60 mg/kg) of hypoxyprobe-1 (pimonidazole HCl). After that, the mice were sacrificed by cervical dislocation to abruptly cut off the blood circulation. Then the chests were opened, and the hearts were removed immediately for dissection. The hearts were sectioned at 4μm intervals and labeled with rabbit anti-hypoxyprobe antibody (PAb2627AP), which is included in the kit, followed by labeling with an Alexa-Fluor-conjugated secondary antibody. Co-injection of hypoxyprobe with lectin was performed as follows: 1 hour before sacrifice, the mice were intraperitoneally injected with hypoxyprobe-1; and 5 min before sacrifice, the mice were tail intravenously injected with lectin. Hearts collected and stained as above.

Histological and immunofluorescence staining

Tissue sections were fixed in precooled 4% paraformaldehyde for 15 min and then washed with phosphate-buffered saline (PBS) for 3 min, three times. The sections were blocked with 2% bovine serum albumin (BSA) for 1 h at 37°C. Primary antibodies were incubated at 37°C for 1 h, followed by incubation at 4°C overnight. The primary antibodies used were as follows: TNNI3 (ab56357, Abcam, 1:200), RFP (600-401-379,

Rockland, 1:1000), PECAM1 (AF3628, R&D, 1:100), VEGFR2 (9698, Cell Signaling Technology, 1:100), VE-cadherin (ab33168, Abcam, 1:200), and HIF-1α (AF1935, R&D, 1:100). After incubation, the sections were washed with PBS for 10 min, three times. Then, the secondary antibodies were incubated at 37℃ for 1 h at a concentration of 1/1000. The secondary antibodies used were as follows: Alexa Fluor 488 goat anti-mouse (Thermo Fisher, A-11001), Alexa Fluor 488 donkey anti-goat (Thermo Fisher, A-11055), Alexa Fluor 488 goat anti-rabbit (Thermo Fisher, A-11008), Alexa Fluor 568 goat anti-rabbit (Thermo Fisher, A-11011), and Alexa Fluor 647 chicken anti-rabbit (Thermo Fisher, A-21443). Nuclei were counterstained with 4′,6-diamidino-2-phenylindole dihydrochloride (DAPI, Sigma, D9542). The blank control was incubated with 2% BSA instead of primary antibodies. All sections were examined by a laser confocal microscopy (ECLIPSE Ti A1, Nikon). All sections were taken approximately 100 μm below the ligature, and at least three fields for each section were captured for each animal unless specifically mentioned.

Apoptosis detection

EC apoptosis was detected *in situ* using a terminal deoxynucleotidyl transferase-mediated dUTP-biotin nick end-labeling assay (TUNEL; 11767305001, Roche, USA) following the manufacturer's instructions. Briefly, the tissue sections were fixed with 4% paraformaldehyde for 15 min, washed with PBS for 3 min, two times and treated with a precooled permeabilization solution (0.1% Triton X-100) for 2 min. After washing with PBS for 3 min, two times, the labeling reaction was carried out in a solution containing terminal deoxynucleotidyl transferase and fluorescein-dUTP at 37°C for 1 h. Nuclei were counterstained with 4′,6-diamidino-2-phenylindole dihydrochloride (DAPI, Sigma, D9542). TUNEL staining was examined by a laser confocal microscope (ECLIPSE Ti A1, Nikon).

Measurement of blood perfusion

Fifty micrograms of fluorescein isothiocyanate (FITC)-labeled *Lycopersicon esculentum* (tomato) lectin (MP6311, MKbio) diluted in 100 μL of sterilized PBS was injected into the mice through the tail vein 5 min before sacrifice according to a previous study.[2] Heart tissues were embedded in optimal cutting temperature compound gel (Leica, Germany), frozen in liquid nitrogen, and cut into 5 or 100 μm sections for visualization of blood infusion and three-dimensional (3D) construction using a laser confocal microscope (ECLIPSE Ti A1, Nikon). The ischemic area (IA) was recognized by a reduction in lectin infusion compared with the sham-operated control. The percentage of lectin-positive volume relative to the total tissue volume indicates the extent of blood perfusion for each sample, and was calculated using ImageJ.

Statistical analysis

ImageJ was applied to analyze the stained images. All data are presented as the mean ± SD. GraphPad Prism 7.0 was applied to perform statistical analysis. Two-way analysis of variance (ANOVA) was used to evaluate different times after LAD ligation and sham operation, and Student's *t*-test was used to compare the difference between the MI group and the sham-operated group. The value $p < 0.05$ was considered statistically significant.

Results

Hypoxic location in the subendocardial region of ischemic myocardium

Overall, there was a significant loss of cardiomyocytes, as detected by HE staining (see Figure 1(a)) and cardiomyocyte-specific marker TNNI3 (Cardiac Troponin I Type 3) staining (see Figure 1(b)) after MI. However, cardiomyocytes in the subendocardial region of the ischemic myocardium survived from day 1 to day 7 post ischemia (see Figure 1). The use of a hypoxyprobe determined that the hypoxic transition took place right after ischemia, sustained on day 1 post ischemia, and declined thereafter (see Figure 2). Importantly, in the subendocardial region, the hypoxyprobe binding was mostly located at the boundary of areas occupied by surviving cardiomyocytes (see Figure 2). Correspondingly, staining for the key hypoxia-responsive transcription factor (hypoxia-inducible factor-1 alpha, HIF-1α) showed that HIF-1α was less detectable in the subendocardial region compared to the other regions of the IA (see Supplemental Figure 1).

Transformation of ECs in the subendocardium after ischemic insults

We determined the changes of a selective protein of ECs, PECAM1 (see Figure 3). Reduced PECAM1⁺ ECs (see Figure 3(a) and (b)) and downregulation of PECAM1 expression (see Figure 3(a) and (c)) were observed in the ischemic myocardium on day 1 post MI, whereas PECAM1 expression was recovered on day 4 and 7 post MI (see Figure 3(c)). VEGFR2, another EC marker, was also dramatically decreased on day 1 post MI (see Supplemental Figure 2). In contrast to the depressed EC selective marker proteins, TUNEL staining indicated that the ECs in the subendocardial region did not undergo apoptosis (see Figure 3(d) to (f)).

To investigate whether the suppression of EC marker proteins results from a reduction of the number of ECs or from the reduced expression in the same ECs, we used *Tie2*ᵗᵈᵀᵒᵐᵃᵗᵒ transgenic mice, in which ECs were specifically labeled by red fluorescent protein (see Figure 4(a), Supplemental Figures 3 and 4). It was observed that tdTomato-positive ECs (tdTomato⁺ ECs) decreased in most regions of the ischemic myocardium but remained the same in the subendocardial region on day 1 post-MI (see Figure 4(b) and (c)). We then calculated the ratio of PECAM1/tdTomato to reflect the change of the surviving ECs. This ratio was significantly decreased, indicating a transformation from PECAM1⁺ ECs to PECAM1⁻ ECs in the subendocardial region (see Figure 4(d) and (e)). We also examined the EC junction protein, VE-cadherin, which was also decreased. Furthermore, co-immunostaining of VE-cadherin and PECAM1 revealed that these two proteins
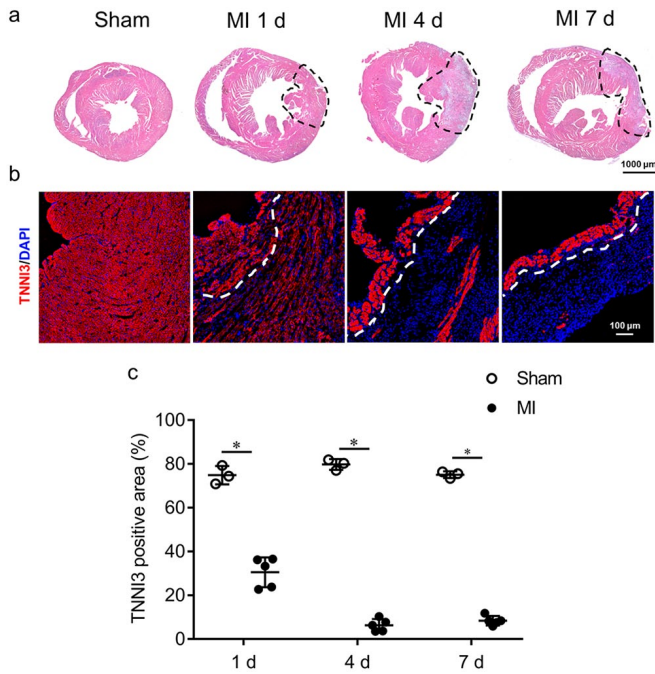
Figure 1. Survival of cardiomyocytes in the subendocardium of ischemic myocardium.
(a) HE staining showed cardiomyocytes in the subendocardium survive from day 1 to day 7 after myocardial ischemia. Scale bar: 1000 μm. (b) Immunofluorescence staining of cardiomyocyte marker TNNI3 (red). Nuclei were stained with DAPI (blue). Scale bar: 100 μm. The subendocardial region in the ischemic area (IA) were indicated by dotted lines. (c) Statistical analysis of TNNI3 positive area (%) in the ischemic area (IA).
Sham: sham-operated control; MI: myocardial ischemia. $n \geqslant 3$ per group; $*p < 0.05$ between indicated groups.
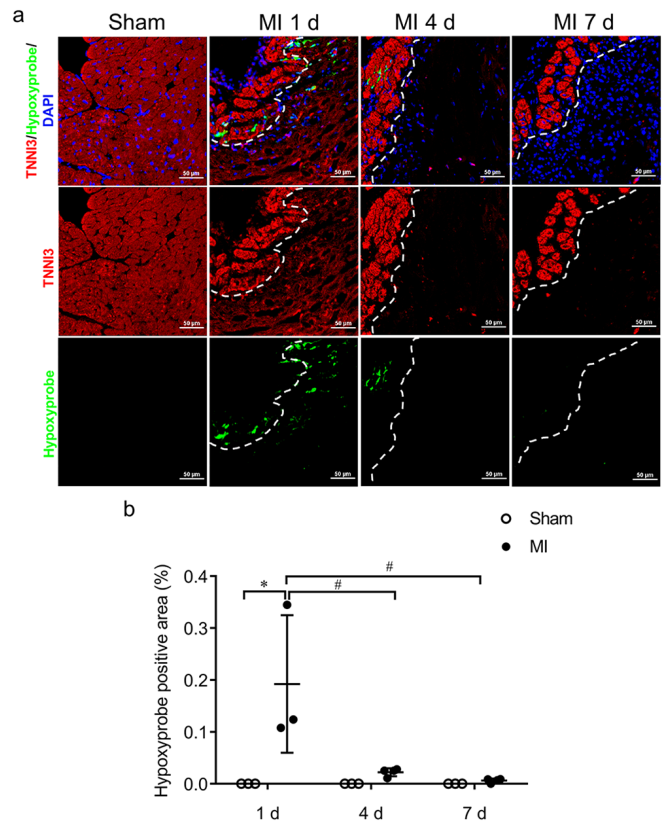

Figure 2. Detection of hypoxyprobe in the subendocardium of ischemic myocardium.
(a) Co-immunofluorescence staining of TNNI3 (red) and hypoxyprobe (green). Nuclei were stained with DAPI (blue). Scale bar: 50 μm. The subendocardial region in the ischemic area (IA) were indicated by dotted lines. (b) Statistical analysis of hypoxyprobe positive area (%) in the ischemic area (IA). Sham: sham-operated control; MI: myocardial ischemia. $n \geqslant 3$ per group; $*p < 0.05$ comparing sham with MI groups; $\#p < 0.05$ comparing MI 1 day with MI 4 or 7 days.

became disassociated in the ischemic myocardium, in contrast to being co-localized in the sham-operated controls (see Figure 4(f) and (g)).

Blood infiltration in the subendocardial region of ischemic myocardium

With regard to the changes of the endothelial junction, we detected blood infiltration in the subendocardial region of the ischemic myocardium. Intravenous injection of FITC-lectin was used to reflect blood perfusion. LAD coronary artery ligation blocked FITC-lectin perfusion to most IAs on day 1 post MI, with the exception of the subendocardial region of the ischemic myocardium (see Figure 5(a) to (c)), indicating an increase in the permeability of the vasculature in the subendocardial region. Co-injection of hypoxyprobe with FITC-lectin revealed that the blood-infiltrated subendocardial region was much less hypoxic on day 1 post MI, as evidenced by the separation of the lectin perfusion area and the hypoxyprobe binding area (see Figure 5(d)).

Discussion

Cardiomyocyte survival in the subendocardial region of ischemic myocardium has been observed in human[18,19] and animal models.[3,4,7,20] Previous studies have shown that

preservation of the functional microvascular bed is vital for the long-term survival of cardiomyocytes.[4] However, the reasons these cardiomyocytes may escape ischemic injury have not been elucidated. This study used transgenic mice with EC-specific labeling and investigated the role of endothelial alterations in cardiomyocyte survival. The study identified a reservation of ECs in the subendocardial region during the early stage of MI, which underwent a transformation with an increase in their permeability. This allowed blood infiltration and created a unique microenvironment, ensuring the survival of cardiomyocytes in the subendocardium under ischemic conditions.

ECs are major constituents of blood vessels, play a vital role in the physiological function of blood vessels, and require a precise coordination of multiple functional proteins.[21–23] In response to ischemic injury, ECs display various gene expression signatures, as currently revealed by single cell RNA sequencing.[24] These changes are associated with EC activation and the release of proteases, which in turn degrade the ECM and contribute to the ECM remodeling.[25] We found that during the ECM remodeling, LOX plays a critical role in collagens
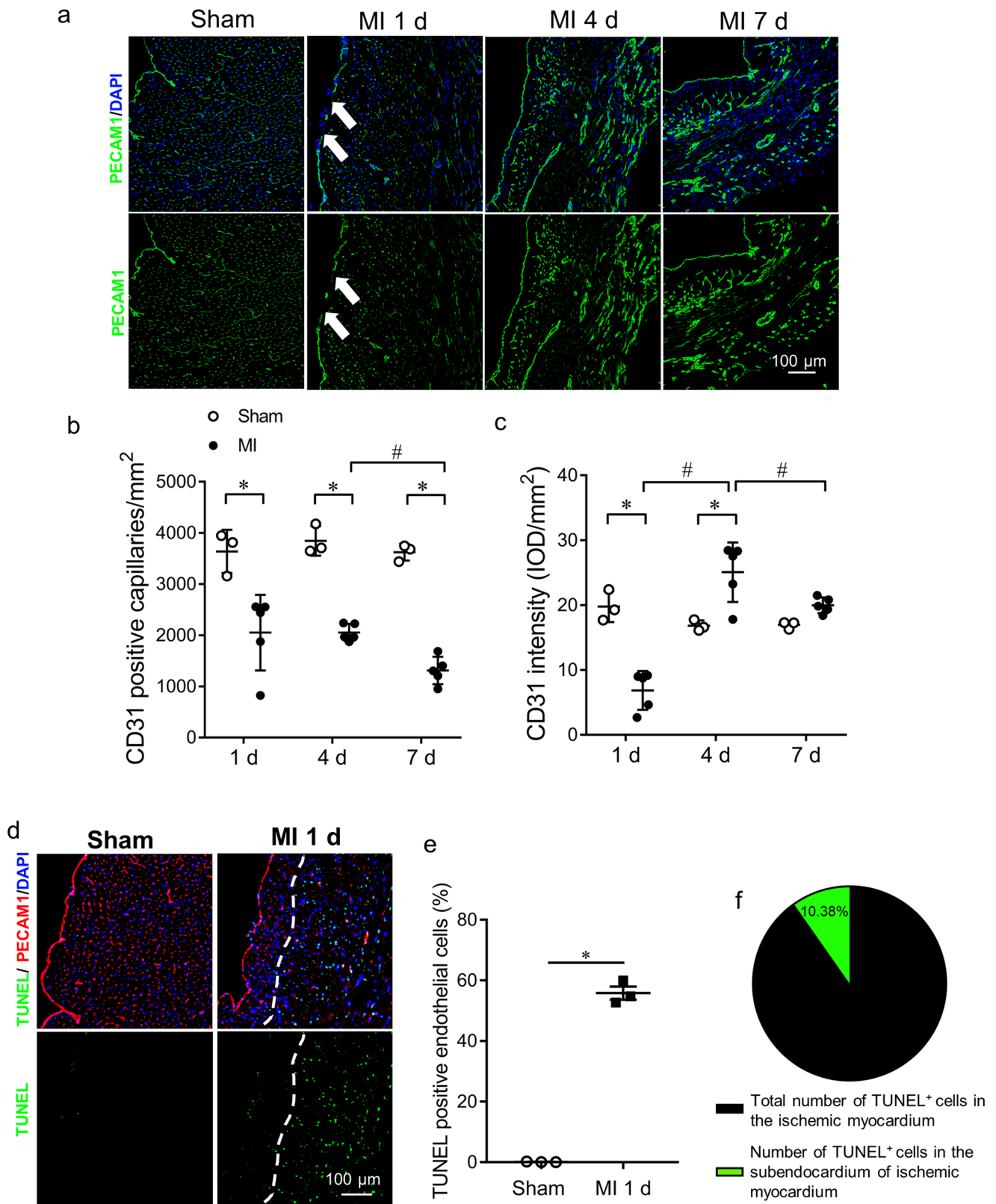
Figure 3. Decrease in endothelial cells after ischemic insults.
(a) Immunofluorescence staining of PECAM1 (green). Nuclei were stained with DAPI (blue). Scale bar: 100 µm. White arrows indicated endocardial leakage on MI 1 day. (b) Statistical analysis of PECAM1+ capillaries per mm². $n \geqslant 3$ per group; *$p < 0.05$ comparing sham with MI groups; #$p < 0.05$ comparing MI 4 days with MI 7 days. (c) Statistical analysis of PECAM1 intensity. $n \geqslant 3$ per group; *$p < 0.05$ comparing sham with MI groups; #$p < 0.05$ comparing MI 1 day with MI 4 days and comparing MI 4 days with MI 7 days. IOD: integrated optical density. (d) TUNEL assay combined with PECAM1 (red) staining on 1 day after myocardial ischemia. Scale bar, 100 µm. The subendocardial region in the ischemic area (IA) was indicated by a dotted line. (e) Statistical analysis of TUNEL+ endothelial cells (%) in the IA of the myocardium. $n \geqslant 3$ per group; *$p < 0.05$ between indicated groups. (f) Pie chart of the percentage of TUNEL+ cells in the subendocardium versus the total number of TUNEL+ cells in the IA of the myocardium. $n \geqslant 3$ per group. Sham: sham-operated control; MI: myocardial ischemia.
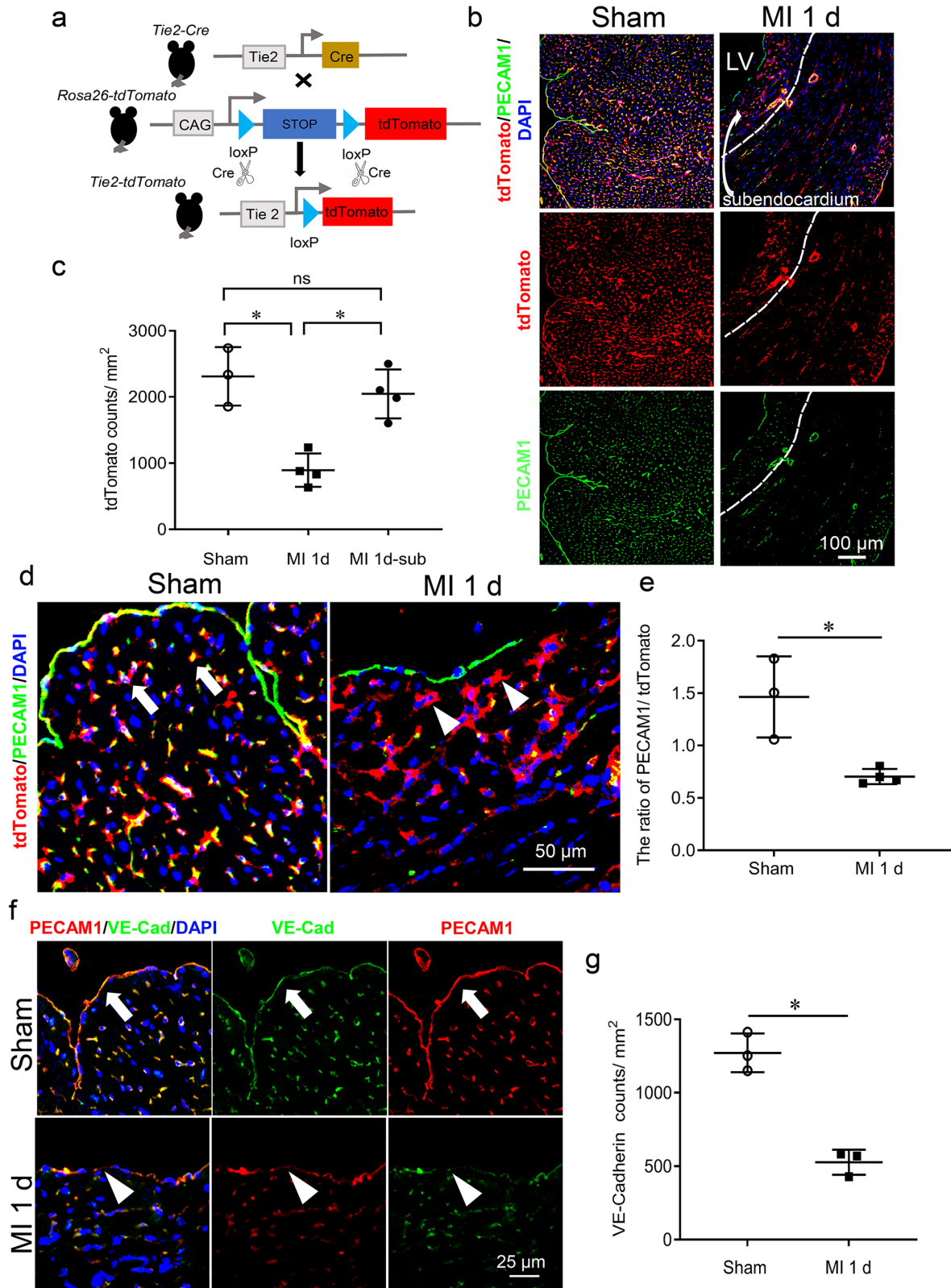
Figure 4. Reservation of endothelial cells and changes in the endocardial junction in the subendocardium of ischemic myocardium.
(a) Schematic diagram of *Tie2*[tdTomato] transgenic mice generated by *Tie2Cre; Rosa26-tdTomato* mice. (b) Co-immunofluorescence staining of PECAM1 (green) and tdTomato (red). Nuclei were stained with DAPI (blue). Scale bar: 100 μm. The subendocardial region in the ischemic area (IA) was indicated by a dotted line. LV: left ventricle. (c) Statistical analysis of tdTomato counts per mm². $n \geqslant 3$ per group; *$p < 0.05$ between indicated groups. MI 1 d-Sub: MI 1 day-subendocardium, the subendocardial region in the IA on MI day 1. (d) Localization of tdTomato (red) and PECAM1 (green) by high magnification imaging. Scale bar: 50 μm. White arrows indicated tdTomato[+]PECAM1^{+} endothelial cells in the sham group. White arrowheads indicated tdTomato[+]PECAM1^{-} endothelial cells in MI 1 d group. (e) Statistical analysis of PECAM1/tdTomato ratio. $n \geqslant 3$ per group; *$p < 0.05$ between indicated groups. (f) Co-immunofluorescence staining of VE-cadherin (green) and PECAM1 (red). Nuclei were stained with DAPI (blue). Scale bar, 25 μm. White arrows indicated co-localization of VE-cadherin and PECAM1, whereas white arrowheads indicated dissociation of VE-cadherin and PECAM1 in the endocardium of the ischemic myocardium. (g) Statistical analysis of VE-cadherin counts per mm². Sham: sham-operated control; MI: myocardial ischemia; VE-Cad: VE-cadherin. $n \geqslant 3$ per group; *$p < 0.05$ between indicated groups.
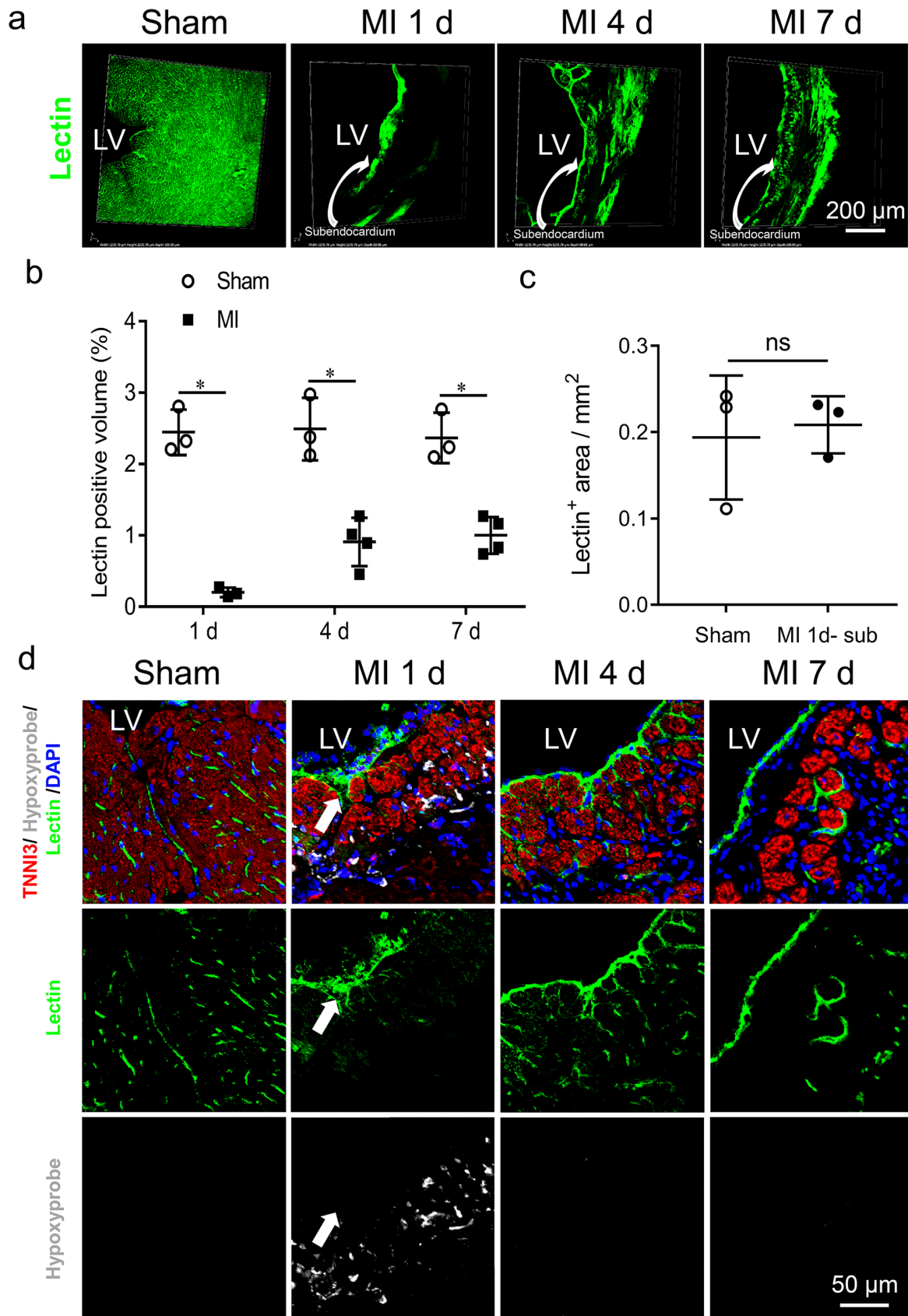
Figure 5. Changes in blood supply in the subendocardial region of ischemic myocardium.
(a) 3D images of lectin perfusion. Scale bar: 200 μm. LV: left ventricle. (b) Statistical analysis of lectin-positive volume normalized to total tissue volume. $n \geqslant 3$ per group; $*p < 0.05$ between the indicated groups. (c) Statistical analysis of lectin-positive area per mm². $n \geqslant 3$ per group; ns, no significance between Sham and MI 1 d-Sub. MI 1 d-Sub: MI 1 day-subendocardium, the subendocardial region in the ischemic area on MI day 1. (d) FITC-lectin (green) combined with a hypoxyprobe (white) to show the correlation between blood perfusion and hypoxic area. Cardiomyocytes were stained with TNNI3 (red) and nuclei were with DAPI (blue). Scale bar: 50 μm. $n \geqslant 3$ per group. White arrows indicated lectin perfusion to nourish the surviving cardiomyocytes on MI 1 day, and showed the separation of the lectin perfusion area and the hypoxyprobe binding area. LV: left ventricle; Sham: sham-operated control; MI: myocardial ischemia.

deposition and reorganization.[3] On the contrary, ECM remodeling can alter the mechanical properties of the tissue and lead to changes in EC shape and migration, contributing to the formation of new blood vessels and the recovery of injured myocardium.[26,27] In addition, ECM remodeling can affect the expression of EC surface molecules, which can alter EC adhesion.[28,29] Understanding the dynamic changes of ECs and ECM remodeling in response to ischemic injury is important for the development of new therapeutic strategies for the treatment of heart diseases.[30,31]

Here, we observed changes in critical proteins in ECs, leading to an increase in vasculature permeability in the subendocardial region of the ischemic myocardium. ECs cover the cardiac chamber, which regulate vascular barrier function and control the passage of plasma proteins and circulating cells across the endothelium.[9,32] Dysregulation of endothelial permeability is associated with many diseases, including inflammation and edema.[33] Thus, endothelial permeability is tightly controlled by numerous extracellular components and mediators to maintain tissue homeostasis.[34,35] PECAM1, also known as CD31, belongs to the immunoglobulin family and is a critical component of the ECM for ECs, regulating the cell–cell interactions.[16] Studies have also revealed many other functions of PECAM1, including acting as a receptor in response to shear stress and mediating neutrophil adhesion.[36,37]

In this study, we observed that PECAM1 was significantly decreased after ischemic insult, but ECs remained viable in the subendocardial region of the ischemic myocardium. Previous studies found that the loss of PECAM1 disrupts the blood–brain barrier (BBB), allowing T-cell trafficking to the central nervous system in multiple sclerosis.[38] We found that PECAM1 partially disappeared, thus leaving an endothelial gap and a disruption of the EC junction in the endocardium. VE-cadherin is another important component of EC junctions,[34,39] and its concomitant depression with the reduction in PECAM1 in the surviving ECs further indicates the disruption of EC junctions in the subendocardial region. As the pathological process progresses, angiogenesis occurs in the ischemic myocardium, which can partially compensate for the reduced blood supply.[28,31] The restoration of blood supply might help to restore the expression of PECAM1 in ECs, leading to the recovery of endothelial permeability. Thus, the dynamic change in endothelial permeability and blood infiltration in the subendocardial region nourishes cardiomyocytes and ensures their survival in the early stage of MI.

Apoptotic cells were rarely detected in the subendocardial region, and this might be related to the unique microenvironment of the subendocardial region.[3] Although PECAM1 depression can cause EC apoptosis,[40] we did not observe an association between PECAM1 depression and EC apoptosis on day 1 after ischemic insult in the subendocardial region. Thus, increased permeability of ECs due to the disruption of the cell–cell conjunction would be responsible for blood infiltration for the survival of cardiomyocytes in this region. VEGFR2 is a receptor corresponding to VEGF that activates cell proliferation and growth.[17] We found that VEGFR2 was dramatically depressed in the surviving ECs, suggesting a limited EC proliferation in the early stage of ischemia.

Changes in surviving ECs and thereafter an increase in the permeability of the vasculature would therefore constitute a mechanism for the survival of cardiomyocytes in the subendocardial region. On the contrary, cardiomyocytes not only survive in the microenvironment supported by ECs, but also in turn promote angiogenesis through paracrine effects under the ischemic condition.[41] Thus, cardioprotective cross-talk between cardiomyocytes and ECs ensures the continuous progression of myocardial regeneration.[42] This endogenous self-rescuing mechanism for cardiomyocytes in the subendocardial region should be further investigated for a better understanding of myocardial regeneration.

In summary, we demonstrate that there are surviving but transformed ECs in the subendocardial region in response to ischemic insult, leading to an increased permeability of the vasculature to allow blood infiltration. This blood infiltration improves the microenvironment, likely leading to the survival of cardiomyocytes in the subendocardial region of the ischemic myocardium. This self-rescuing mechanism for myocardial survival from ischemic injury can therefore be considered great importance for an understanding of myocardial regeneration.

ORCID ID

Y James Kang https://orcid.org/0000-0001-8449-7904

SUPPLEMENTAL MATERIAL

Supplemental material for this article is available online.

REFERENCES

1. Konijnenberg LSF, Damman P, Duncker DJ, Kloner RA, Nijveldt R, van Geuns RM, Berry C, Riksen NP, Escaned J, van Royen N. Pathophysiology and diagnosis of coronary microvascular dysfunction in ST-elevation myocardial infarction. *Cardiovasc Res* 2020;**116**:787–805

2. Xiao Y, Song X, Wang T, Meng X, Feng Q, Li K, Kang YJ. Copper preserves vasculature structure and function by protecting endothelial cells from apoptosis in ischemic myocardium. *J Cardiovasc Transl Res* 2021;**14**:1146–55

3. Chu Q, Xiao Y, Song X, Kang YJ. Extracellular matrix remodeling is associated with the survival of cardiomyocytes in the subendocardial region of the ischemic myocardium. *Exp Biol Med (Maywood)* 2021;**246**:2579–88

4. Nofi C, Bogatyryov Y, Dedkov EI. Preservation of functional microvascular bed is vital for long-term survival of cardiac myocytes within large transmural post-myocardial infarction scar. *J Histochem Cytochem* 2018;**66**:99–120

5. Brutsaert DL. Cardiac endothelial-myocardial signaling: its role in cardiac growth, contractile performance, and rhythmicity. *Physiol Rev* 2003;**83**:59–115

6. Colliva A, Braga L, Giacca M, Zacchigna S. Endothelial cell-cardiomyocyte crosstalk in heart development and disease. *J Physiol* 2020;**598**:2923–39

7. Xie Y, Chen J, Han P, Yang P, Hou J, Kang YJ. Immunohistochemical detection of differentially localized up-regulation of lysyl oxidase and down-regulation of matrix metalloproteinase-1 in rhesus monkey model of chronic myocardial infarction. *Exp Biol Med (Maywood)* 2012;**237**:853–9

8. Sturtzel C. Endothelial cells. *Adv Exp Med Biol* 2017;**1003**:71–91

9. Kalucka J, de Rooij L, Goveia J, Rohlenova K, Dumas SJ, Meta E, Conchinha NV, Taverna F, Teuwen LA, Veys K, Garcia-Caballero M, Khan S, Geldhof V, Sokol L, Chen R, Treps L, Borri M, de Zeeuw P, Dubois C, Karakach TK, Falkenberg KD, Parys M, Yin X, Vinckier S, Du Y, Fenton RA, Schoonjans L, Dewerchin M, Eelen G, Thienpont B, Lin L, Bolund L, Li X, Luo Y, Carmeliet P. Single-cell transcriptome atlas of murine endothelial cells. *Cell* 2020;**180**:764–79.e20

10. Heitzer T, Schlinzig T, Krohn K, Meinertz T, Munzel T. Endothelial dysfunction, oxidative stress, and risk of cardiovascular events in patients with coronary artery disease. *Circulation* 2001;**104**:2673–8

11. Simoons ML, Serruys PW, van den Brand M, Res J, Verheugt FW, Krauss XH, Remme WJ, Bär F, de Zwaan C, van der Laarse A, Vermeer F, Lubsen J. Early thrombolysis in acute myocardial infarction: limitation of infarct size and improved survival. *J Am Coll Cardiol* 1986;**7**:717–28

12. Chin SP, Maskon O, Tan CS, Anderson JE, Wong CY, Hassan HHC, Choor CK, Fadilah SAW, Cheong SK. Synergistic effects of intracoronary infusion of autologous bone marrow-derived mesenchymal stem cells and revascularization procedure on improvement of cardiac function in patients with severe ischemic cardiomyopathy. *Stem Cell Investig* 2021;**8**:2

13. Sun X, Wu J, Qiang B, Romagnuolo R, Gagliardi M, Keller G, Laflamme MA, Li RK, Nunes SS. Transplanted microvessels improve pluripotent stem cell-derived cardiomyocyte engraftment and cardiac function after infarction in rats. *Sci Transl Med* 2020;**12**:eaax2992

14. Lertkiatmongkol P, Liao D, Mei H, Hu Y, Newman PJ. Endothelial functions of platelet/endothelial cell adhesion molecule-1 (CD31). *Curr Opin Hematol* 2016;**23**:253–9

15. Nukala SB, Regazzoni L, Aldini G, Zodda E, Tura-Ceide O, Mills NL, Cascante M, Carini M, D'Amato A. Differentially expressed proteins in primary endothelial cells derived from patients with acute myocardial infarction. *Hypertension* 2019;**74**:947–56

16. Newman PJ, Berndt MC, Gorski J, White GC II, Lyman S, Paddock C, Muller WA. PECAM-1 (CD31) cloning and relation to adhesion molecules of the immunoglobulin gene superfamily. *Science* 1990;**247**:1219–22

17. Simons M, Gordon E, Claesson-Welsh L. Mechanisms and regulation of endothelial VEGF receptor signalling. *Nat Rev Mol Cell Biol* 2016;**17**:611–25

18. Forman R, Cho S, Factor SM, Kirk ES. Acute myocardial infarct extension into a previously preserved subendocardial region at risk in dogs and patients. *Circulation* 1983;**67**:117–24

19. López B, Querejeta R, González A, Beaumont J, Larman M, Díez J. Impact of treatment on myocardial lysyl oxidase expression and collagen cross-linking in patients with heart failure. *Hypertension* 2009;**53**:236–42

20. Li C, Peng H, Kang YJ. Cardiomyocyte-specific COMMD1 deletion suppresses ischemia-induced myocardial apoptosis. *Cardiovasc Toxicol* 2021;**21**:572–81

21. Tian X, Pu WT, Zhou B. Cellular origin and developmental program of coronary angiogenesis. *Circ Res* 2015;**116**:515–30

22. Eklund L, Kangas J, Saharinen P. Angiopoietin-Tie signalling in the cardiovascular and lymphatic systems. *Clin Sci (Lond)* 2017;**131**:87–103

23. Nesmith JE, Chappell JC, Cluceru JG, Bautch VL. Blood vessel anastomosis is spatially regulated by Flt1 during angiogenesis. *Development* 2017;**144**:889–96

24. Tombor LS, John D, Glaser SF, Luxan G, Forte E, Furtado M, Rosenthal N, Baumgarten N, Schulz MH, Wittig J, Rogg EM, Manavski Y, Fischer A, Muhly-Reinholz M, Klee K, Looso M, Selignow C, Acker T, Bibli SI, Fleming I, Patrick R, Harvey RP, Abplanalp WT, Dimmeler S. Single cell sequencing reveals endothelial plasticity with transient mesenchymal activation after myocardial infarction. *Nat Commun* 2021;**12**:681

25. Takawale A, Zhang P, Azad A, Wang W, Wang X, Murray AG, Kassiri Z. Myocardial overexpression of TIMP3 after myocardial infarction exerts beneficial effects by promoting angiogenesis and suppressing early proteolysis. *Am J Physiol Heart Circ Physiol* 2017;**313**:H224–36

26. Wang X, Khalil RA. Matrix metalloproteinases, vascular remodeling, and vascular disease. *Adv Pharmacol* 2018;**81**:241–330

27. Xiao Y, Liu Y, Liu J, Kang YJ. The association between myocardial fibrosis and depressed capillary density in rat model of left ventricular hypertrophy. *Cardiovasc Toxicol* 2018;**18**:304–11

28. Wu X, Reboll MR, Korf-Klingebiel M, Wollert KC. Angiogenesis after acute myocardial infarction. *Cardiovasc Res* 2021;**117**:1257–73

29. Mougin Z, Huguet Herrero J, Boileau C, Le Goff C. ADAMTS proteins and vascular remodeling in aortic aneurysms. *Biomolecules* 2021;**12**:12

30. Prabhu SD, Frangogiannis NG. The biological basis for cardiac repair after myocardial infarction: from inflammation to fibrosis. *Circ Res* 2016;**119**:91–112

31. Lupu IE, De Val S, Smart N. Coronary vessel formation in development and disease: mechanisms and insights for therapy. *Nat Rev Cardiol* 2020;**17**:790–806

32. Marin-Juez R, El-Sammak H, Helker CSM, Kamezaki A, Mullapuli ST, Bibli SI, Foglia MJ, Fleming I, Poss KD, Stainier DYR. Coronary revascularization during heart regeneration is regulated by epicardial and endocardial cues and forms a scaffold for cardiomyocyte repopulation. *Dev Cell* 2019;**51**:503–15.e4

33. Park-Windhol C, D'Amore PA. Disorders of vascular permeability. *Annu Rev Pathol* 2016;**11**:251–81

34. Rho SS, Ando K, Fukuhara S. Dynamic regulation of vascular permeability by vascular endothelial cadherin-mediated endothelial cell-cell junctions. *J Nippon Med Sch* 2017;**84**:148–59

35. Cerutti C, Ridley AJ. Endothelial cell-cell adhesion and signaling. *Exp Cell Res* 2017;**358**:31–8

36. Collins C, Osborne LD, Guilluy C, Chen Z, O'Brien ET III, Reader JS, Burridge K, Superfine R, Tzima E. Haemodynamic and extracellular matrix cues regulate the mechanical phenotype and stiffness of aortic endothelial cells. *Nat Commun* 2014;**5**:3984

37. Winneberger J, Schöls S, Lessmann K, Rández-Garbayo J, Bauer AT, Mohamud Yusuf A, Hermann DM, Gunzer M, Schneider SW, Fiehler J, Gerloff C, Gelderblom M, Ludewig P, Magnus T. Platelet endothelial cell adhesion molecule-1 is a gatekeeper of neutrophil transendothelial migration in ischemic stroke. *Brain Behav Immun* 2021;**93**:277–87

38. Wimmer I, Tietz S, Nishihara H, Deutsch U, Sallusto F, Gosselet F, Lyck R, Muller WA, Lassmann H, Engelhardt B. PECAM-1 stabilizes blood-brain barrier integrity and favors paracellular T-cell diapedesis across the blood-brain barrier during neuroinflammation. *Front Immunol* 2019;**10**:711

39. Giannotta M, Trani M, Dejana E. VE-cadherin and endothelial adherens junctions: active guardians of vascular integrity. *Dev Cell* 2013;**26**:441–54

40. Brown S, Heinisch I, Ross E, Shaw K, Buckley CD, Savill J. Apoptosis disables CD31-mediated cell detachment from phagocytes promoting binding and engulfment. *Nature* 2002;**418**:200–3

41. Gladka MM, Kohela A, Molenaar B, Versteeg D, Kooijman L, Monshouwer-Kloots J, Kremer V, Vos HR, Huibers MMH, Haigh JJ, Huylebroeck D, Boon RA, Giacca M, van Rooij E. Cardiomyocytes stimulate angiogenesis after ischemic injury in a ZEB2-dependent manner. *Nat Commun* 2021;**12**:84

42. Bloomekatz J, Galvez-Santisteban M, Chi NC. Myocardial plasticity: cardiac development, regeneration and disease. *Curr Opin Genet Dev* 2016;**40**:120–30